Evaluation of Apparent Diffusion Coefficient Thresholds for Diagnosis of Medulloblastoma Using Diffusion-Weighted Imaging

THEODORE THOMAS PIERCE[1], JAMES M. PROVENZALE[2,3]

[1] Duke University School of Medicine; Durham, NC, USA
[2] Department of Radiology, Duke University Medical Center; Durham, NC, USA, [3] Departments of Radiology and Imaging Sciences, Oncology and Biomedical Engineering, Emory University School of Medicine; Atlanta, GA, USA

Key words: apparent diffusion coefficient, posterior fossa tumor, medulloblastoma, computer-assisted diagnosis

SUMMARY – *We assess a diffusion-weighted imaging (DWI) analysis technique as a potential basis for computer-aided diagnosis (CAD) of pediatric posterior fossa tumors. A retrospective medical record search identified 103 children (mean age: 87 months) with posterior fossa tumors having a total of 126 preoperative MR scans with DWI. The minimum ADC (ADC_{min}) and normalized ADC (nADC) values [ratio of ADC_{min} values in tumor compared to normal tissue] were measured by a single observer blinded to diagnosis. Receiver operating characteristic (ROC) curves were generated to determine the optimal threshold for which the nADC and ADC_{min} values would predict tumor histology. Inter-rater reliability for predicting tumor type was evaluated using values measured by two additional observers. At histology, ten tumor types were identified, with astrocytoma (n=50), medulloblastoma (n=33), and ependymoma (n=9) accounting for 89%. Mean ADC_{min} (0.54×10^{-3} mm^2/s) and nADC (0.70) were lowest for medulloblastoma. Mean ADC_{min} (1.28×10^{-3} mm^2/s) and nADC (1.64) were highest for astrocytoma. For the ROC analysis, the area under the curve when discriminating medulloblastoma from other tumors using nADC was 0.939 and 0.965 when using ADC_{min}. The optimal ADC_{min} threshold was 0.66×10^{-3} mm^2/s, which yielded an 86% positive predictive value, 97% negative predictive value, and 93% accuracy. Inter-observer variability was very low, with near perfect agreement among all observers in predicting medulloblastoma. Our data indicate that both ADC_{min} and nADC could serve as the basis for a CAD program to distinguish medulloblastoma from other posterior fossa tumors with a high degree of accuracy.*

Introduction

The term computer-assisted diagnosis (CAD), when applied to imaging studies, refers to the use of artificial intelligence to produce computerized schemes for detection and characterization of lesions in radiologic images [1]. This technique relies on computers to analyze diagnostic imaging and provide radiologists with clinically relevant information. Extensive literature describes the implementation of CAD for detection and diagnosis of a number of conditions including pulmonary nodules, breast cancer, and aneurysms [2,3]. However, applications of CAD to neuroradiology, and in particular, to brain tumor diagnosis, have been relatively limited to date [4-6]. The goal of the present study was to test an analytic technique based on diffusion-weighted imaging for classification of pediatric posterior fossa tumors that might be amenable to eventual automated use via CAD.

The information provided by conventional magnetic resonance (MR) imaging is often insufficient to accurately and consistently differentiate the three most common pediatric posterior fossa tumors, i.e., medulloblastoma, ependymoma, and cerebellar astrocytoma [7]. Although each tumor has certain characteristic

features, heterogeneity in imaging appearance limits confident diagnosis in many cases. For example, all three tumors can present in the midline, have cystic and enhancing solid components, and are relatively common in children around the age of five years old [7]. Distinction of medulloblastoma from ependymoma can be particularly challenging because of their typical location within the fourth ventricle [7].

Diffusion-weighted imaging (DWI) has shown potential for preoperative discrimination of childhood posterior fossa tumors based on apparent diffusion coefficient (ADC) maps [8-11]. Medulloblastomas often exhibit lower rates of microscopic water diffusion (i.e., lower ADC values) than other common posterior fossa tumors of childhood [12-14]. This feature is most likely due to the fact that medulloblastomas are characterized by a high degree of cellularity and often contain cells with a high nuclear:cytoplasmic ratio, which provides an increased number of membrane barriers to microscopic water diffusion [14,15]. While not conclusive, recent work has suggested that ADC maps may be useful to noninvasively diagnose medulloblastoma using this characteristic [8-10,12,13,16-22].

A number of methods exist for measuring water diffusivity in tumors. These methods include measuring the minimum ADC value (hereafter termed ADC_{min}) within the entire tumor [15,18,19], measuring the average ADC value within the entire tumor or within contrast-enhancing portions of tumor [20,23,24], normalizing ADC values within the tumor to those in normal tissue (hereafter referred to as nADC) [8,14,24] and using ADC histograms [12]. Most studies of nADC values are performed in a quantitative manner but some studies have measured nADC values by qualitative visual inspection [17,19]. Each method has shown promise for distinguishing the major pediatric posterior fossa tumors from one another, but these studies have produced conflicting results [8-10,12,13,16-22]. Furthermore, a number are limited by small sample sizes. For instance, although medulloblastoma is a relatively common tumor, numerous studies had fewer than ten medulloblastoma patients enrolled [8,10,13,14,17,20,23,25].

Among the various types of ADC measurements used in previous studies, ADC_{min} and nADC appeared to have the most value [8,24]. In this study, we set out to determine ADC thresholds that could potentially be used in CAD programs that would eventually aid in automated means for specific diagnosis of posterior fossa tumor.

Materials and Methods

Patient Selection

IRB approval was obtained at our university-based, tertiary-care facility and a waiver of informed consent was provided. A retrospective medical record search was performed selecting patients who had pretreatment MR scans using DWI at our institution between January 1, 2001 and December 31, 2011, were 18 years of age or younger at the time of imaging, and had histological verification of a posterior fossa tumor. Our search attempted to identify all tumors that could have an imaging appearance similar to medulloblastoma and the list of search terms included medulloblastoma, ependymoma, astrocytoma, atypical teratoid/rhabdoid tumor, and choroid plexus papilloma; those five tumor types represent the vast majority of pediatric posterior fossa tumors.

Seven hundred and fifty two patients were identified; 367 patients were excluded due to unavailable pathology reports for posterior fossa pathology and another 200 patients were excluded because the patients did not have posterior fossa masses. Eighty-two patients were excluded because they lacked preoperative DWI; the remaining 103 patients (who had a total of 126 preoperative MR scans with DWI imaging) were included in the study. In total, 86 MR scans were performed at our institution and 40 MR scans were performed elsewhere. We performed an analysis using one scan per patient, i.e., 103 MR scans in 103 patients and in that sample, 75 scans were from our institution and 28 were from other institutions.

Image Analysis

All scans included unenhanced and contrast-enhanced axial T1-weighted images, T2-weighted images, fluid-attenuated inversion recovery (FLAIR) images and DWI images. ADC maps were provided as part of the MR scan on our PACS system in 91 cases and ADC map analysis was performed on that workstation. In the remaining 35 cases, solely DWI images (and not ADC maps) were provided with the MR scan. In those cases, ADC maps were created and analyzed using the Functool ADC program on a GE Advantage Workstation version 4.4.

A single observer (hereafter referred to as rater 1) examined all ADC maps and specifically sought the lowest ADC values within the

tumor. The placement of regions of interest (ROIs) in all cases was later verified by a neuroradiologist with 20 years of clinical experience and, when necessary, ROIs were placed in a more appropriate location. Both individuals were blinded to histological diagnosis. Circular 30 mm^2 ROIs, similar in size to those used by other investigators [18,21,26] were placed on the three sites having the lowest ADC values. ROIs were placed without overlap with one another. Fewer ROIs were permitted for very small tumors, which was necessitated in MR scans in six patients. ROI placement was guided by the fact that the regions with lowest ADC values are typically the darkest regions within the tumor on the ADC map. Thus, the initial placement of ROIs was guided by visual inspection to determine the regions of lowest signal intensity. Thereafter, the observer interrogated these regions to find the sites of lowest ADC values. In order to decrease the likelihood that low signal intensity regions represented areas of susceptibility related to hemorrhage or calcification, the ADC maps were simultaneously viewed with images from other pulse sequences and, when available, CT scans. The observer then placed an ROI at each of the three sites with the lowest ADC values. The lowest of these three values, ADC_{min}, was recorded. As an internal reference, a 30 mm^2 ROI was placed in the left putamen and right putamen, after determining that these structures had a normal appearance on other pulse sequences. These values were used to determine the ratio between ADC_{min} and normal tissue, nADC.

Tumor Histology

Pathology reports were obtained using the electronic medical record at our institution. All diagnoses were unequivocal. Using the pathology report, tumors were classified into one of four categories: medulloblastoma, ependymoma, astrocytoma, or other.

Statistical Analysis

Analysis was performed in Rstudio version 0.94.92. Patient characteristics are shown in Table 1 with values represented as means with standard deviation.

The primary analysis examined the utility

Table 1 Patient demographic information and mean DWI characteristics for each tumor type.

Tumor	*Mean (sd) Age (Years)*	*Cases (# male)*	*Mean (sd) $ADC_{min} \times 10^{-3}$ mm^2/s*	*Mean (sd) nADC*
Medulloblastoma	6.4 (4.6)	33 (20)	0.54 (0.09)	0.70 (0.12)
Ependymoma	6.2 (5.3)	9 (8)	0.88 (0.13)	1.16 (0.21)
Astrocytoma	8.0 (5.0)	50 (31)	1.28 (0.32)	1.64 (0.46)
Other*	7.8 (6.7)	11 (7)	0.88 (0.36)	1.16 (0.56)

*Other tumors consisted of atypical teratoid/rhabdoid tumor (n=3), choroid plexus papilloma (n–3), benign choroid plexus mass (n–1), glioblastoma (n=1), high grade teratoma (n=1), malignant glioneuronal tumor (n=1), and Rosai-Dorfman disease (n=1).
The mean and standard deviation of measured minimum tumor ADC (ADC_{min}) for each tumor type is shown in column 4. Medulloblastoma has the lowest mean ADC_{min} while astrocytoma has the highest. The mean ADC ratio (nADC) is shown in column 5 where medulloblastoma is shown as having the lowest value and astrocytoma as having the highest value.

Table 2 Summary of optimal thresholds to discriminate medulloblastoma from solely ependymoma or from all other posterior fossa tumors.

Comparison		*AUC (95% CI)*	*Optimal ADC Threshold*	*Sensitivity*	*Specificity*	*Positive Predictive Value*	*Negative Predictive Value*	*Accuracy*
ADC_{min}	M vs. A	0.965 (0.931-0.999)	0.66 × 10–3 mm2/s	0.939	0.929	0.861	0.970	0.932
	M vs. E	0.990 (0.968-1.000)	0.675 × 10–3 mm2/s	0.970	1.000	1.000	0.900	0.976
nADC	M vs. A	0.939 (0.887-0.991)	0.905	0.970	0.900	0.821	0.984	0.922
	M vs. E	0.983 (0.953-1.000)	1.00	0.970	0.889	0.970	0.889	0.952

Abbreviations: *M*-medulloblastoma, *A*-all other tumors (including ependymoma), *E*-ependymoma.

Medulloblastoma was correctly discriminated from all tumors and from ependymoma alone using minimum tumor ADC (ADC_{min}) and ADC ratio (nADC). Discriminatory ability was analyzed using receiver operating characteristic (ROC) curves. This was quantified using the area under the curve (AUC), for which 1 is a perfect score. Optimal thresholds, calculated by optimizing accuracy, are listed in column 3. Sensitivity, specificity, positive predictive value, negative predictive value, and accuracy are reported for each comparison using the optimal threshold. When distinguishing medulloblastoma from all other tumors, an ADC_{min} greater than 0.66×10^{-3} mm^2/s excluded medulloblastoma in 97% of cases.

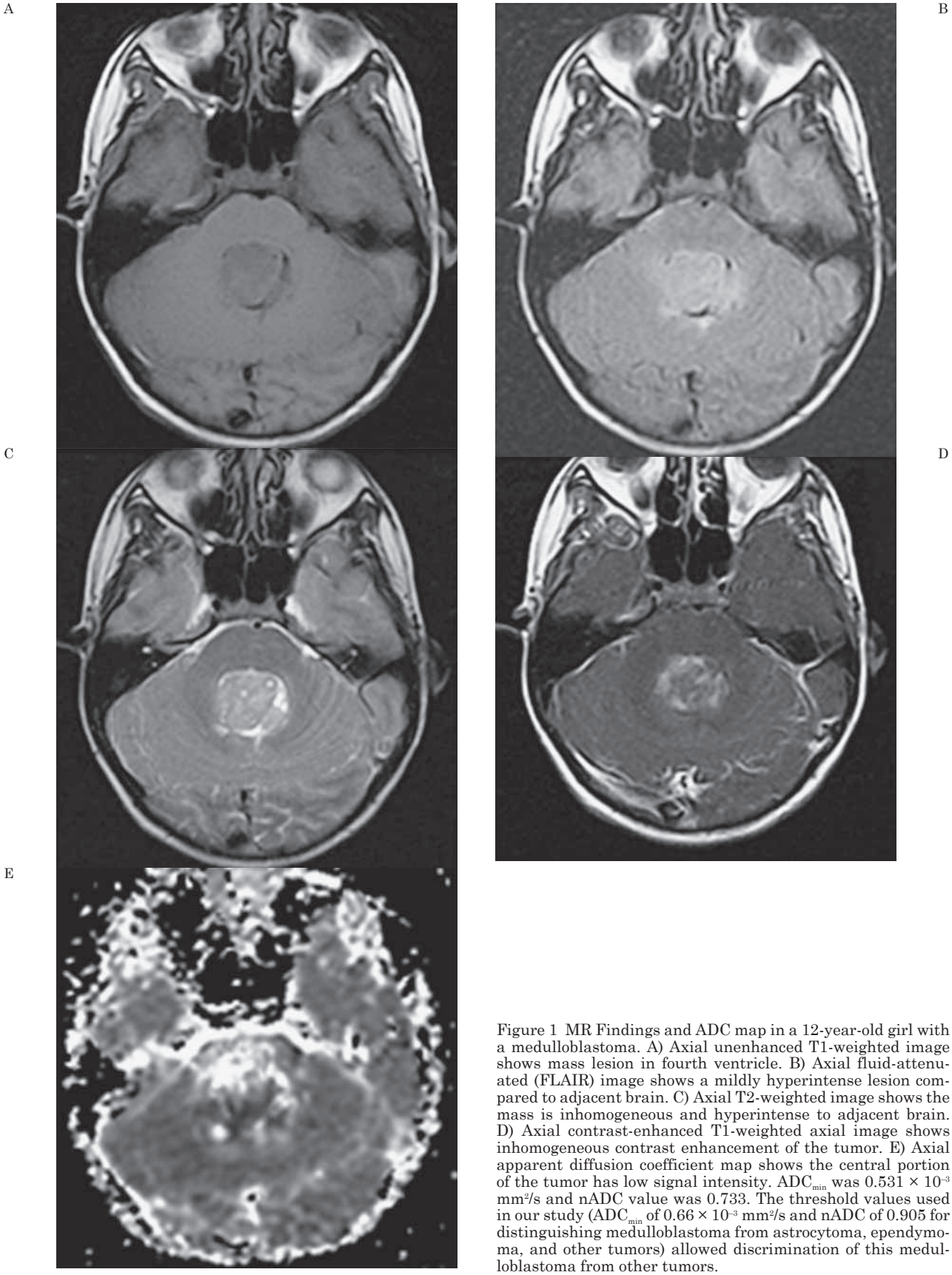

Figure 1 MR Findings and ADC map in a 12-year-old girl with a medulloblastoma. A) Axial unenhanced T1-weighted image shows mass lesion in fourth ventricle. B) Axial fluid-attenuated (FLAIR) image shows a mildly hyperintense lesion compared to adjacent brain. C) Axial T2-weighted image shows the mass is inhomogeneous and hyperintense to adjacent brain. D) Axial contrast-enhanced T1-weighted axial image shows inhomogeneous contrast enhancement of the tumor. E) Axial apparent diffusion coefficient map shows the central portion of the tumor has low signal intensity. ADC_{min} was 0.531×10^{-3} mm^2/s and nADC value was 0.733. The threshold values used in our study (ADC_{min} of 0.66×10^{-3} mm^2/s and nADC of 0.905 for distinguishing medulloblastoma from astrocytoma, ependymoma, and other tumors) allowed discrimination of this medulloblastoma from other tumors.

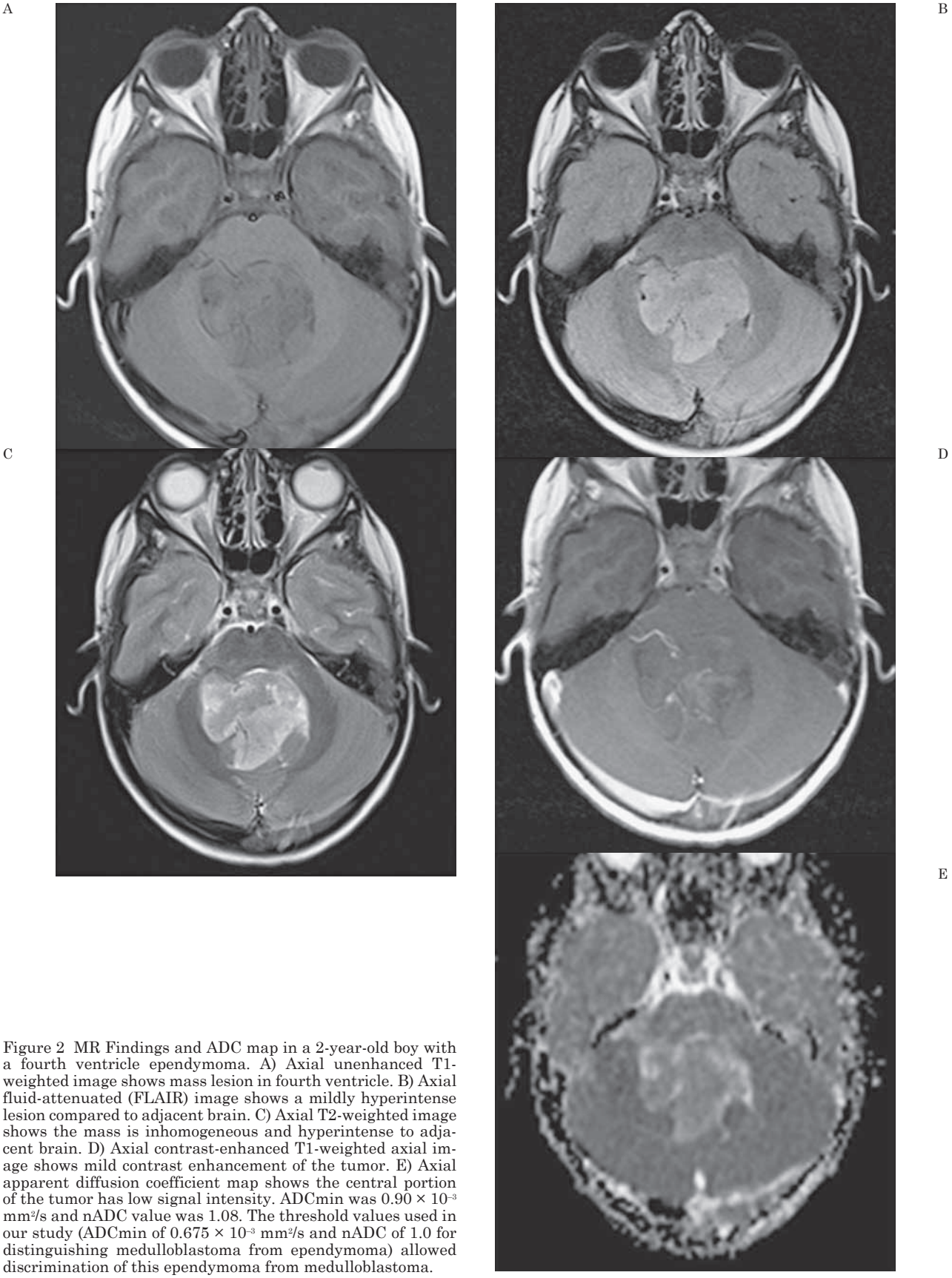

Figure 2 MR Findings and ADC map in a 2-year-old boy with a fourth ventricle ependymoma. A) Axial unenhanced T1-weighted image shows mass lesion in fourth ventricle. B) Axial fluid-attenuated (FLAIR) image shows a mildly hyperintense lesion compared to adjacent brain. C) Axial T2-weighted image shows the mass is inhomogeneous and hyperintense to adjacent brain. D) Axial contrast-enhanced T1-weighted axial image shows mild contrast enhancement of the tumor. E) Axial apparent diffusion coefficient map shows the central portion of the tumor has low signal intensity. ADCmin was 0.90×10^{-3} mm^2/s and nADC value was 1.08. The threshold values used in our study (ADCmin of 0.675×10^{-3} mm^2/s and nADC of 1.0 for distinguishing medulloblastoma from ependymoma) allowed discrimination of this ependymoma from medulloblastoma.

of ADC values in predicting tumor histology. In cases where multiple imaging examinations were available, only the examination directly prior to surgery was used for this purpose. Two primary predictor variables were assessed. Minimum tumor ADC value (ADC_{min}) was defined as the lowest ADC value recorded of the three ADC measurements. The second variable was the ADC ratio (nADC). This was calculated by dividing ADC_{min} by the mean of the two normal tissue ADC values measured in both putamina. We examined two primary outcomes: distinguishing medulloblastoma from all posterior fossa tumors and distinguishing medulloblastoma solely from ependymoma.

Four receiver operating characteristic (ROC) curves were generated to evaluate the performance of ADC_{min} and nADC in distinguishing (1) medulloblastoma from other tumors and (2) medulloblastoma solely from ependymoma. Overall test performance for each of the four comparisons is reported in Table 2 using the area under the curve (AUC). We determined optimal ADC_{min} and nADC thresholds to distinguish medulloblastomas from all tumors and medulloblastomas from ependymomas alone by maximizing accuracy for each comparison. Also reported for each optimal cutoff in Table 2 are sensitivity, specificity, positive predictive value, negative predictive value, and accuracy.

Measurement of Intra-Observer Variability

In order to assess intra-observer variability in distinguishing tumor types, rater 1 performed these measurements a second time in a random sample of 25 patients from the dataset after a delay of four weeks. We then measured the number of discrepant readings between the first reading and the second reading, i.e. the number of cases in which the observer would predict different tumor histology, using the optimal ADC_{min} and nADC thresholds, between the first and second assessment. Agreement was reported using Cohen's kappa statistic.

Measurement of Inter-Observer Variability

To assess the inter-observer variability of the ADC_{min} method, two additional raters (rater 2 and rater 3), both 3rd year medical students blinded to histological diagnosis, were enlisted to measure ADC_{min} within tumors on a GE Advantage Workstation (version 4.4). Six examinations could not be transferred due to incompatible formatting. Raters 2 and 3 assessed the remaining 97 cases by measuring ADC_{min} in a fashion similar to that used by rater 1 except that ROI placement was not supervised by a neuroradiologist. Additionally, normal tissue ADC values used to calculate nADC were not measured. The number of discrepant readings for pairwise comparisons between the three raters was calculated. Discrepant readings were cases in which one observer would predict a different tumor histology, using the optimal ADC_{min} thresholds, compared to a different rater. Agreement was reported using Cohen's kappa statistic for each pairwise rater comparison.

Measures from Repeat Studies

For ADC values to be used for automated diagnosis of posterior fossa tumors, the analysis technique would need to be applicable to a wide variety of scanners. Stated differently, it is important to know if ADC value measurement for predicting tumor type depends on which MR scan is used when multiple scans are available. To address this issue, we measured ADC_{min} values and nADC values for the 12 patients who had multiple pretreatment MR scans and assessed whether determination of tumor type based on our optimal thresholds would differ between MR scans. A total of 35 MR scans existed for these patients, 22 from our institution and 13 from an outside institution.

Results

Pathology

Ten different tumor types were identified. Among these, 50 cases were determined at histology to be astrocytomas, 33 cases were medulloblastomas, and nine were ependymomas. The remaining 11 cases comprised three atypical teratoid/rhabdoid tumors, three choroid plexus papillomas, one benign choroid plexus mass, one glioblastoma, one high-grade teratoma, one malignant glioneuronal mass, and one case of Rosai-Dorfman disease (a lesion characterized by massive histiocytosis which, in our patient, presented as a cerebellar mass and was thought preoperatively to represent a tumor).

ADC measurements

Both mean ADC_{min} (0.54×10^{-3} mm^2/s) and mean nADC (0.70) were lowest for medulloblastoma (Table 1). An example of a medul-

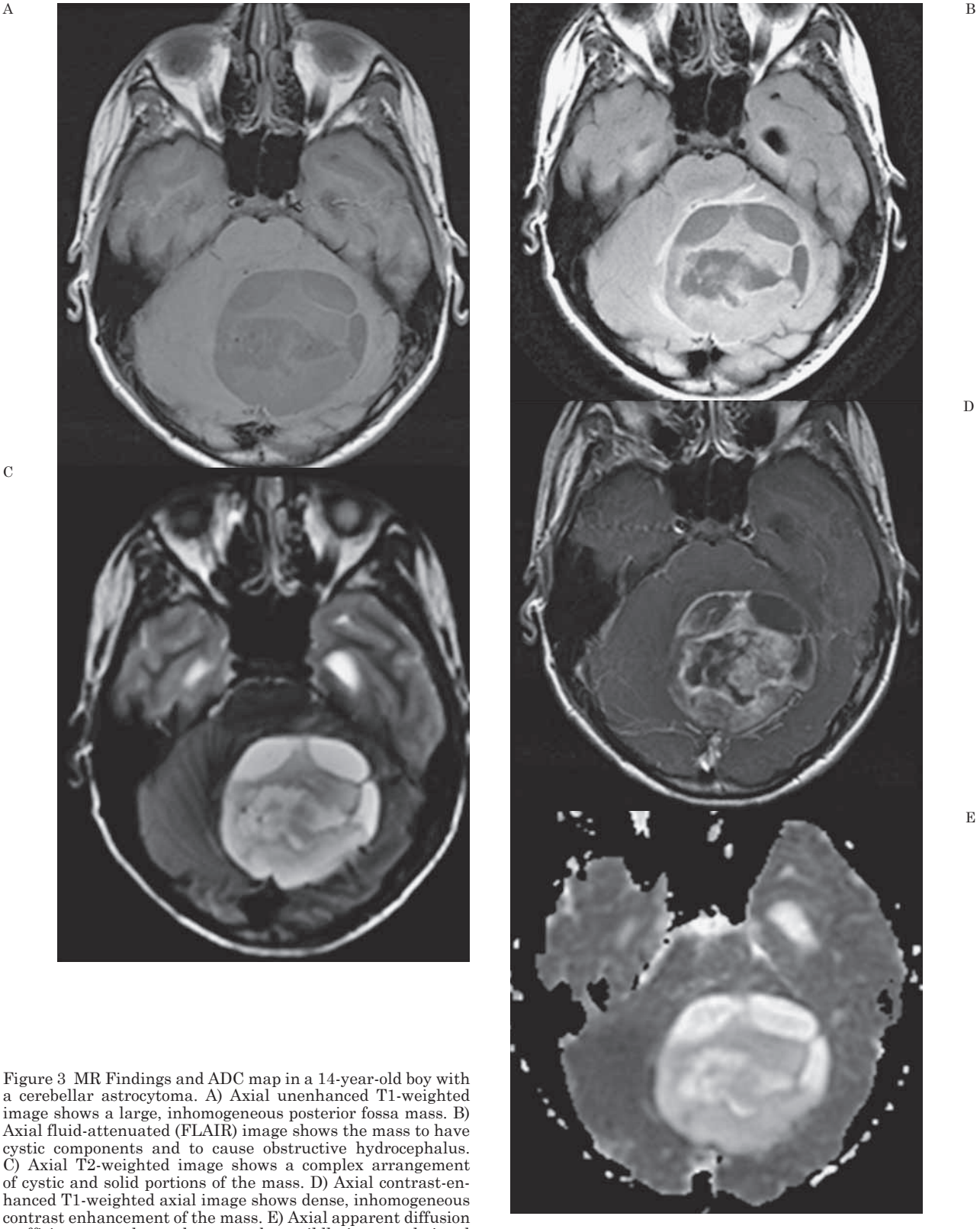

Figure 3 MR Findings and ADC map in a 14-year-old boy with a cerebellar astrocytoma. A) Axial unenhanced T1-weighted image shows a large, inhomogeneous posterior fossa mass. B) Axial fluid-attenuated (FLAIR) image shows the mass to have cystic components and to cause obstructive hydrocephalus. C) Axial T2-weighted image shows a complex arrangement of cystic and solid portions of the mass. D) Axial contrast-enhanced T1-weighted axial image shows dense, inhomogeneous contrast enhancement of the mass. E) Axial apparent diffusion coefficient map shows the tumor has mildly increased signal intensity compared to adjacent normal brain. ADCmin was 1.64×10^{-3} mm²/s and nADC value was 2.03. The threshold values used in our study would correctly predict that this is not a medulloblastoma.

loblastoma is shown in Figure 1, that of an ependymoma in Figure 2 and an astrocytoma in Figure 3. Mean ADC_{min} (1.28×10^{-3} mm²/s)

and mean nADC (1.64) were highest for astrocytoma. Ependymoma and other tumor types each had a mean ADC_{min} of 0.88 10^{-3} mm^2/s and mean nADC of 1.16. Medulloblastoma was the only group to show ADC_{min} less than the ADC of normal tissue, i.e. a nADC less than 1.

Receiver Operating Characteristic Curves

Receiver operating characteristic (ROC) curves using ADC_{min} and nADC to distinguish medulloblastoma from all tumors and solely from ependymomas are shown in Figure 4. AUC was smallest, at 0.939, when distinguishing medulloblastoma from all tumors using nADC, and largest, 0.990, when distinguishing medulloblastoma from ependymoma using ADC_{min}. AUC results for all four comparisons are shown in Table 2, which indicates that ADC_{min} appears to be a slightly better metric than nADC for distinguishing both medulloblastoma from all tumors and medulloblastoma from ependymoma alone. Nonetheless, both metrics appear to be very good for purposes of distinction of the major tumor types. Table 2 also shows the optimal test characteristics for a given threshold chosen by maximizing accuracy. Using an ADC_{min} threshold of 0.66 10^{-3} mm^2/s, low ADC_{min} correctly identified medulloblastoma from all other tumors in 86% of cases while elevated ADC_{min} correctly excluded medulloblastoma in 97% of cases. With regard to specifically distinguishing medulloblastoma from ependymoma, a threshold ADC value of 0.675 10^{-3} mm^2/s properly classified these two tumors in nearly 98% of cases.

Intra-Observer Variability

Single observer repeated measurements in a random sample of tumors showed one discrepant case when distinguishing medulloblastoma from all other tumors using ADC_{min}, yielding a kappa of 0.92. For the remaining comparisons (identifying medulloblastoma from all others using nADC and medulloblastoma from ependymoma using nADC and ADC_{min}) all values were concordant, yielding a kappa of 1 in each instance.

Inter-Observer Variability

The ADC_{min} values for raters 1 and 2 were either both above or both below the threshold value of 0.66×10^{-3} mm^2/s in 96% of cases, indicating that their measurements would predict the same histologic diagnosis in 96% of cases. This produced a kappa value of 0.91. For the combinations of raters 1 and 3 and of raters 2 and 3, concordance was also reached in 96% of cases; in each comparison, the kappa value was 0.90. These findings indicate near perfect agreement among all raters.

Measures from Repeat Studies

The ADC_{min} and nADC values for the 12 patients with multiple preoperative DWI examinations are shown in Figure 5. The histological diagnoses in those patients included astrocytoma (n=9), medulloblastoma (n=1), and glioneuronal neoplasm (n=1, which was categorized as "other"). The magnitude of variation of ADC_{min} and nADC for a given subject naturally differed between patients. Nonetheless, in only one case (with histological diagnosis of astrocytoma) would prediction based on the ADC_{min} and nADC criteria on the first MR scan have differed from that predicted from the second MR scan. Although the initial MR scan, based upon our ADC_{min} and nADC criteria, would have predicted the tumor not be medulloblastoma, values from a second MR scan would have incorrectly predicted the mass to be a medulloblastoma.

Discussion

The goal of this study was to evaluate ADC_{min} and nADC as metrics for distinguishing medulloblastoma from other posterior fossa tumors in the hope that these metrics could serve as the basis for eventual use in CAD of posterior fossa tumors. For such use to be possible, it is mandatory that ADC_{min} and nADC be highly reproducible for the purpose of discriminating tumor types. Although these values were solely helpful in predicting medulloblastoma (as opposed to other posterior fossa tumors), the results were indeed highly reproducible in that capacity, with little inter-observer variability even using a manual technique. The results would be expected to be at least as good using a program that scanned ADC values in a tumor in an automated manner. Even though our analysis did not provide a means to distinguish all other pediatric posterior fossa tumors from one another, it is feasible that DWI metrics could be used in conjunction with other imaging characteristics in a CAD program to help radiologists more accurately determine tumor

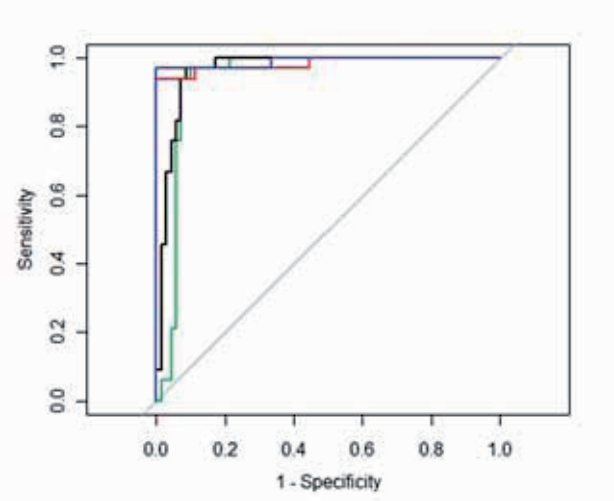

Figure 4 Receiver operating characteristics (ROC) curve for correct identification of medulloblastoma. The ROC curve for medulloblastoma identified from ependymoma using minimum tumor ADC (ADCmin) shown in blue and ADC ratio (nADC) shown in red. ROC curve for medulloblastoma identified from all tumors using ADC_{min} is shown in black and nADC is shown in green. Medulloblastoma is correctly identified more often when using ADCmin versus nADC.

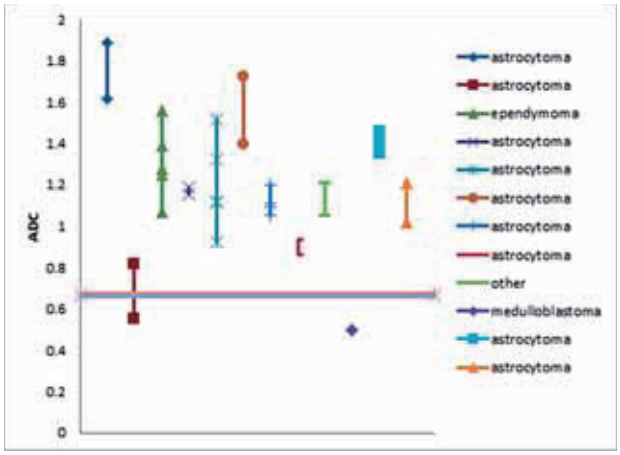

Figure 5 Similarity of ADCmin measurements obtained on serial MR examinations. Minimum tumor ADC (ADCmin) values are plotted for each patient with multiple DWI examinations. Only one patient had variation in ADC_{min} that would have crossed the threshold shown as a horizontal line. Thus only one case would be categorized differently using ADCmin based upon the time of imaging. No general trend of ADCmin variation was seen over time.

type. In fact, such studies using artificial neural networks to characterize brain tumors are already underway for adult brain tumors [5]. As an example, investigators are assessing pattern classification methods for discriminating between primary gliomas and metastases, as well as grading primary brain tumors [6]. Thus, larger studies encompassing greater numbers of pediatric fossa brain tumors, incorporating additional imaging features other than solely the ADC values used in our study, might produce a means to better discriminate between all tumors.

We found that both metrics provided a means to distinguish medulloblastoma from other posterior fossa tumors with a high degree of accuracy. The ADC_{min} method was shown to identify medulloblastoma with a high degree of accuracy (93.2% when compared to all other tumors and 97.6% when compared solely to ependymoma, the other major fourth ventricular tumor). More importantly, ADC_{min} used as a diagnostic test had a high positive predictive and negative predictive value, which is of particular relevance to clinical radiologists in interpreting radiological studies. For example, 97% of all posterior fossa tumors, regardless of other factors, with an ADC_{min} greater than 0.66 × 10^{-3} mm^2/s were not medulloblastoma. Combined with other relevant clinical and radiological findings, ADC_{min} would likely have even greater power to correctly predict tumor histology prior to surgery. We will test the ability of our ADC thresholds against the ability of neuroradiologists to correctly diagnose posterior fossa tumors in a future study.

Measurement of Both ADC Values and nADC for Distinguishing Tumor Types

Although, to the best of our knowledge, no studies have compared ADC_{min} values and nADC for distinguishing posterior fossa tumors, our review of the medical literature did show three articles in which nADC values and mean ADC values (as opposed to ADC_{min}) were measured (but not compared) [8,14,24]. In one report, mean ADC values in medulloblastomas (0.66 × 10^{-3} mm^2/s) were significantly lower than in ependymomas (1.10 × 10^{-3} mm^2/s); an ADC threshold value of 0.90 × 10^{-3} mm^2/s was sufficient for distinction of the two tumors (as opposed to the minimum ADC value [i.e., ADC_{min}] threshold of 0.675 × 10^{-3} mm^2/s in our study) [8]. In addition, those authors calculated nADC values using the mean ADC value, whereas we calculated nADC values using ADC_{min}. In that study, the mean nADC value for medulloblastoma was 0.84 (as opposed to 0.70 using ADC_{min} in our study) and was significantly different from that of ependymoma, which was 1.39 (compared to 1.16 in our study). In another re-

port, the investigators found substantial overlap between ADC values of medulloblastomas and ependymomas and were unable to establish a threshold value that would distinguish these tumors [24]. However, in that study, the mean nADC value for medulloblastoma using the thalamus as the reference standard was 0.88 (compared to 0.70 in our study) and for ependymoma was 1.40 (compared to 1.16 in our study). In part, differences in nADC values between our findings and those two studies may be attributable to the fact that we measured the minimum ADC value within tumors (as opposed to the mean ADC value), which would provide a lower ratio when compared against normal brain. Finally, in one report which measured mean ADC values and nADC (using contralateral normal brain as control), the average nADC value in two medulloblastomas was 1.07; no ependymomas were assessed in that series [14].

Our procedure to identify ADC_{min} involves placing an ROI within multiple regions of the tumor, especially those regions that appear hypodense on the ADC map, until the minimum ADC value is obtained. We measured ADC_{min}, as opposed to mean ADC values, in order to avoid the confounding feature of the large degree of tumor heterogeneity due to such factors as cystic areas [18]. This system has the advantages of excluding measurement of cystic and edematous regions, which typically have elevated ADC, as well as being more objective than subjectively determining a representative region of tumor and measuring ADC values within it. Measurement of mean ADC values or ADC_{min} values can allow unintended inclusion of normal tissue as well as regions of calcification and hemorrhage (that can contribute markedly reduced ADC values). Not surprisingly, in some studies, use of the mean ADC value resulted in substantial overlap between ADC values of various tumor types and a relative inability to discriminate tumor types [18].

ADC_{min} values for analysis of tumors have been employed by other investigators [15,19]. For instance, in one small study, the authors found significant differences between ADC_{min} of medulloblastoma (0.54×10^{-3} mm²/s) and that of ependymoma (0.91×10^{-3} mm²/s) [15]. In another study, use of ADC_{min} values discriminated medulloblastomas (0.67×10^{-3} mm²/s) from low-grade ependymomas (1.11×10^{-3} mm²/s) [19]. Notably, in one study, considerable overlap was seen between ADC_{min} of medulloblastoma and that of ependymoma [18]; the authors did not provide an explanation as to why their results differed from most studies.

Our analysis also assessed normalizing tumor ADC by using the ratio of tumor ADC to normal tissue ADC, which has been studied by some other investigators [8,25]. This procedure would overcome a systematic bias within a scan such as differences between MRI scanners. We tested the influence of scans from multiple institutions in our study by studying the 12 patients who had scans performed at multiple institutions. Only one of these cases would have had different diagnoses predicted based on the scans from two different institutions. In that single case, the nADC value provided the same diagnosis as the ADC_{min} value on each scan. Since the ADC_{min} provides the same diagnosis as nADC and given its slightly greater ease of use, ADC_{min} alone is sufficient to predict tumor histology, even when analyzing cases from multiple institutions and MR scanners. However, future, larger prospective studies would be needed to confirm this conclusion.

In our study, we found only one tumor type with similar DWI characteristics to medulloblastoma, i.e. atypical teratoid/rhabdoid tumor, an uncommon tumor that occurs in the posterior fossa in children and histologically simulates medulloblastoma [26]. In fact, the similarity in water diffusivity characteristics between atypical teratoid/rhabdoid tumors and medulloblastoma has been noted in other studies [8,14,15,27], which can be explained by the similar cellularity characteristics of these tumors [14,15]. In practical terms, the two tumors can usually be distinguished by location and age at presentation. About one half of atypical teratoid/rhabdoid tumors are in the supratentorial compartment whereas medulloblastoma is a posterior fossa tumor; approximately two thirds of infratentorial atypical teratoid/rhabdoid tumors are located in the cerebellopontine angle as opposed to medulloblastomas which, in children, occur in the fourth ventricle in approximately 80% of cases [28]. Age at presentation also differs between the two tumors. Atypical teratoid/rhabdoid tumors usually present within the first 18 months of life whereas medulloblastoma presents over a much broader age range, with a mean age in the range of five to nine years [27,29,30]. Furthermore, about half of atypical rhabdoid tumors have hemorrhagic components (compared with approximately 5% of medulloblastomas). Nonetheless, on the occasions when a non-hemorrhagic atypical teratoid/rhabdoid tumor is located in the fourth ventricle, ADC

values are not likely to be able to distinguish the lesion from medulloblastoma.

Few studies investigating water diffusivity characteristics in pediatric brain tumors have measured positive predictive value and negative predictive value, which are key elements in clinical practice. In one study, Ji et al. categorized tumors as either low-grade (n=49) or high-grade (n=29), a composite of medulloblastoma and high-grade ependymoma [19]. Forty-seven percent of the low-grade tumors were ependymomas and 25% were pilocytic astrocytomas, while 90% of the high-grade tumors were medulloblastomas; thus, the distribution of tumors was relatively similar to our study. The authors used an ADC_{min} threshold of 0.90 mm^2/s to discriminate high-grade tumors from low-grade tumors (rather than specific tumor types), which yielded a positive predictive value of 97% and negative predictive value of 98%. This positive predictive value is somewhat higher than the 87% positive predictive value (for an ADC_{min} threshold of 0.66 mm^2/s for discriminating medulloblastoma from all tumors in our series), but the negative predictive value is essentially the same as in our series (i.e., 97%). Differences between the study of Ji et al. and our study are likely related to differences in study design. While that study defined the outcome of interest as identifying medulloblastoma or high-grade ependymoma from other tumors, we sought to identify only medulloblastomas from other tumors. High-grade ependymomas with restricted diffusion would be regarded as true positives by Ji et al. but as false positives in our study, leading to a reduced positive predictive value. Our lower ADC_{min} threshold reflects this difference in outcomes.

Our techniques can be easily implemented because many institutions already regularly perform DW imaging thus additional imaging time will not be required. Additionally, 32% of the MR scans in our patients were from outside institutions having a wide variety of MR scanners suggesting that the results are not scanner or institution-dependent. Finally, our ADC_{min} method is simple, easy to use, and relatively reproducible such that it may be possible to incorporate this method into a CAD algorithm or a manual rater-based system.

One potential study limitation is that our investigation is retrospective in nature. Major problems of retrospective studies include recall bias (which is not an issue in our study) and selection bias, which can produce an incorrect assessment of relative disease frequency, a feature to which positive and negative predictive values are sensitive. We attempted to minimize misrepresentation of any one tumor incidence (which could bias our results) by including all pediatric posterior fossa tumors evaluated at our tertiary care institution. In fact, the disease incidence observed within this study is similar to previous reports [7]. Thus, it appears likely that the positive predictive value and negative predictive value reported here are applicable to other institutions with similar proportions of astrocytomas, medulloblastomas, and ependymomas. Importantly, a prospective study design would not necessarily have avoided selection bias because no guarantee exists that all presenting patients would be included. Another factor that justifies a retrospective study of pediatric posterior fossa tumors is the relatively low incidence of such tumors, which precludes a single center prospective study; the time to achieve a sufficiently large sample would be impractical. Although a multicenter trial would allow faster patient enrollment, such a study would be costly and challenging to implement. Thus, a reasonable argument can be made that a retrospective study design is appropriate for our study.

One objection that might be introduced with regard to our study is that specific noninvasive diagnosis of tumor type is not important for pediatric posterior fossa tumors because all such lesions will be surgically resected. However, our study is intended to advance the state of knowledge that would be needed to advance the field of CAD in tumor assessment generally. The use of ADC values to distinguish tumor types could well serve not solely to make a specific diagnosis of tumor type but also to assign tumor grading, assess tumor response and distinguish tumors from those entities that mimic tumors [6]. The DWI metrics we evaluated provided a threshold of values that were highly reliable in distinguishing medulloblastomas from other posterior fossa tumors. Predictions made using this threshold were highly reproducible among observers. Thus, these metrics have a potential role in tumor assessment as CAD programs for brain lesion classification develop. Although in our study these metrics could not reliably distinguish other pediatric posterior fossa tumor types from one another, it seems feasible that, when other imaging characteristics are taken into account, a program to better distinguish such tumors could be developed with the aid of CAD.

References

1 Doi K, MacMahon H, Katsuragawa S, et al. Computer-aided diagnosis in radiology: potential and pitfalls. Eur J Radiol. 1999; 31 (2): 97-109. doi: 10.1016/S0720-048X(99)00016-9.
2 Doi K. Computer-aided diagnosis in medical imaging: historical review, current status and future potential. Comput Med Imaging Graph. 2007; 31 (4-5): 198-211. doi: 10.1016/j.compmedimag.2007.02.002.
3 Eadie LH, Taylor P, Gibson AP. A systematic review of computer-assisted diagnosis in diagnostic cancer imaging. Eur J Radiol. 2012; 81 (1): e70-76. doi: 10.1016/j.ejrad.2011.01.098.
4 Emblem KE, Nedregaard B, Hald JK, et al. Automatic glioma characterization from dynamic susceptibility contrast imaging: brain tumor segmentation using knowledge-based fuzzy clustering. J Magn Reson Imaging. 2009; 30 (1): 1-10. doi: 10.1002/jmri.21815.
5 Yamashita K, Yoshiura T, Arimura H, et al. Performance evaluation of radiologists with artificial neural network for differential diagnosis of intra-axial cerebral tumors on MR images. Am J Neuroradiol. 2008; 29 (6): 1153-1158. doi: 10.3174/ajnr.A1037.
6 Zacharaki EI, Wang S, Chawla S, et al. Classification of brain tumor type and grade using MRI texture and shape in a machine learning scheme. Magn Reson Med. 2009; 62 (6): 1609-1618. doi: 10.1002/mrm.22147.
7. Poretti A, Meoded A, Huisman TA. Neuroimaging of pediatric posterior fossa tumors including review of the literature. J Magn Reson Imaging. 2012; 35 (1): 32-47. doi: 10.1002/jmri.22722.
8 Rumboldt Z, Camacho DL, Lake D, et al. Apparent diffusion coefficients for differentiation of cerebellar tumors in children. Am J Neuroradiol. 2006; 27 (6): 1362-1369.
9 Yamasaki F, Kurisu K, Satoh K, et al. Apparent diffusion coefficient of human brain tumors at MR imaging. Radiology. 2005; 235 (3): 985-991. doi: 10.1148/radiol.2353031338.
10 Chen Z, Ma L, Lou X, et al. Diagnostic value of minimum apparent diffusion coefficient values in prediction of neuroepithelial tumor grading. J Magn Reson Imaging. 2010; 31 (6): 1331-1338. doi: 10.1002/jmri.22175.
11 Le Bihan D, Turner R, Douek P, et al. Diffusion MR imaging: clinical applications. Am J Roentgenol. 1992; 159 (3): 591-599. doi: 10.2214/ajr.159.3.1503032
12 Bull JG, Saunders DE, Clark CA. Discrimination of paediatric brain tumours using apparent diffusion coefficient histograms. Eur Radiol. 2012; 22 (2): 447-457. doi: 10.1007/s00330-011-2255-7.
13 Humphries PD, Sebire NJ, Siegel MJ, et al. Tumors in pediatric patients at diffusion-weighted MR imaging: apparent diffusion coefficient and tumor cellularity. Radiology. 2007; 245 (3): 848-854. doi: 10.1148/radiol.2452061535.
14 Gauvain KM, McKinstry RC, Mukherjee P, et al. Evaluating pediatric brain tumor cellularity with diffusion-tensor imaging. Am J Roentgenol. 2001; 177 (2): 449-454. doi: 10.2214/ajr.177.2.1770449.
15 Yamashita Y, Kumabe T, Higano S, et al. Minimum apparent diffusion coefficient is significantly correlated with cellularity in medulloblastomas. Neurol Res. 2009; 31 (9): 940-946. doi: 10.1179/174313209X382520.
16 Higano S, Yun X, Kumabe T, et al. Malignant astrocytic tumors: clinical importance of apparent diffusion coefficient in prediction of grade and prognosis. Radiology. 2006; 241 (3): 839-846. doi: 10.1148/radiol.2413051276.
17 Kan P, Liu JK, Hedlund G, et al. The role of diffusion-weighted magnetic resonance imaging in pediatric brain tumors. Childs Nerv Syst. 2006; 22 (11): 1435-1439. doi: 10.1007/s00381-006-0229-x.
18 Jaremko JL, Jans LB, Coleman LT, et al. Value and limitations of diffusion-weighted imaging in grading and diagnosis of pediatric posterior fossa tumors. Am J Neuroradiol. 2010; 31 (9): 1613-1616. doi: 10.3174/ajnr.A2155.
19 Ji YM, Geng DY, Huang BC, et al. Value of diffusion-weighted imaging in grading tumours localized in the fourth ventricle region by visual and quantitative assessments. J Int Med Res. 2011; 39 (3): 912-919. doi: 10.1177/147323001103900325.
20 Schneider JF, Viola A, Confort-Gouny S, et al. Infratentorial pediatric brain tumors: the value of new imaging modalities. J Neuroradiol. 2007; 34 (1): 49-58. doi: 10.1016/j.neurad.2007.01.010.
21 Lee EJ, Lee SK, Agid R, et al. Preoperative grading of presumptive low-grade astrocytomas on MR imaging: diagnostic value of minimum apparent diffusion coefficient. Am J Neuroradiol. 2008; 29 (10): 1872-1877. doi: 0.3174/ajnr.A1254.
22 Pillai S, Singhal A, Byrne AT, et al. Diffusion-weighted imaging and pathological correlation in pediatric medulloblastomas-"They are not always restricted!". Childs Nerv Syst. 2011; 27 (9): 1407-1411. doi: 10.1007/s00381-011-1499-5.
23 Rodallec M, Colombat M, Krainik A, et al. Diffusion-weighted MR imaging and pathologic findings in adult cerebellar medulloblastoma. J Neuroradiol. 2004; 31 (3): 234-237. doi: 10.1016/S0150-9861(04)97000-9.
24 Gimi B, Cederberg K, Derinkuyu B, et al. Utility of apparent diffusion coefficient ratios in distinguishing common pediatric cerebellar tumors. Acad Radiol. 2012; 19 (7): 794-800. doi: 10.1016/j.acra.2012.03.004.
25 Quadery FA, Okamoto K. Diffusion-weighted MRI of haemangioblastomas and other cerebellar tumours. Neuroradiology. 2003; 45 (4): 212-219. doi: 10.1007/s00234-003-0951-y.
26 Burger PC, Yu IT, Tihan T, et al. Atypical teratoid/rhabdoid tumor of the central nervous system: a highly malignant tumor of infancy and childhood frequently mistaken for medulloblastoma: a Pediatric Oncology Group study. Am J Surg Pathol. 1998; 22 (9): 1083-1092.
27 Koral K, Gargan L, Bowers DC, et al. Imaging characteristics of atypical teratoid-rhabdoid tumor in children compared with medulloblastoma. Am J Roentgenol. 2008; 190 (3): 809-814. doi: 10.2214/AJR.07.3069.
28 Fruehwald-Pallamar J, Puchner SB, Rossi A, et al. Magnetic resonance imaging spectrum of medulloblastoma. Neuroradiology. 2011; 53 (6): 387-396. doi: 10.1007/s00234-010-0829-8.
29 Zhang R, Zhou L. Medulloblastoma. Chin Med J. 1999; 112 (4): 297-301.
30 Modha A, Vassilyadi M, George A, et al. Medulloblastoma in children--The Ottawa experience. Childs Nerv Syst. 2000; 16 (6): 341-350. doi: 10.1007/s003810050529.

James Provenzale, MD
Duke University Medical Center
Department of Radiology and Imaging Sciences
Emory University
DUMC 3808 Durham, NC 27710, USA
Tel.: 919 684 7409
Fax: 919 684 7168
E-mail: James.provenzale@duke.edu